Enantioseparation of Mandelic Acid Enantiomers With Magnetic Nano-Sorbent Modified by a Chiral Selector

TUBA TARHAN,[1,2] BILSEN TURAL,[1]* SERVET TURAL,[1] AND GIRAY TOPAL[1]
[1]*Department of Chemistry, Faculty of Education, Dicle University, Diyarbakir, Turkey*
[2]*Vocational High School of Health Services, Mardin Artuklu University, Mardin, Turkey*

ABSTRACT In this study, *R*(+)-α-methylbenzylamine-modified magnetic chiral sorbent was synthesized and assessed as a new enantioselective solid phase sorbent for separation of mandelic acid enantiomers from aqueous solutions. The chemical structures and magnetic properties of the new sorbent were characterized by vibrating sample magnetometry, transmission electron microscopy, Fourier transform infrared spectroscopy, and dynamic light scattering. The effects of different variables such as the initial concentration of racemic mandelic acid, dosage of sorbent, and contact time upon sorption characteristics of mandelic acid enantiomers on magnetic chiral sorbent were investigated. The sorption of mandelic acid enantiomers followed a pseudo-second-order reaction and equilibrium experiments were well fitted to a Langmuir isotherm model. The maximum adsorption capacity of racemic mandelic acid on to the magnetic chiral sorbent was found to be 405 mg g^{-1}. The magnetic chiral sorbent has a greater affinity for (*S*)-(+)-mandelic acid compared to *(R)-(−)*-mandelic acid. The optimum resolution was achieved with 10 mL 30 mM of racemic mandelic acid and 110 mg of magnetic chiral sorbent. The best percent enantiomeric excess values (up to 64%) were obtained by use of a chiralpak AD-H column. *Chirality 00:000–000, 2015*.

KEY WORDS: resolution; enantioselective sorption; mandelic acid enantiomers; magnetic chiral nanoparticles; isotherm; kinetic

Mandelic acid is an alpha-hydroxy acid obtained from bitter almonds. The (*R*)-form acts as a key intermediate in the production of semisynthetic penicillins and cephalosporins. At the same time, it is used as a chiral synthone and chiral resolving agent in the synthesis of antitumor and antiobesity agents.[1] The (*S*)-form is an important starting material for stereoselective transformations and a versatile intermediate for pharmaceuticals.[2] Also, the (*R*)-form has been used in dermatology, treatment of skin disorders, skin care products, skin inflammation, and resolving redness, for many years.

The enantiopure chiral compounds can be obtained by asymmetric synthesis,[3] fractional crystallization,[4] or chiral chromatography.[5] Separations of enantiomers by chromatography on chiral stationary phases is a widely established methodology for both industry and academia.[6–8]

In recent years, nanoparticles have received more and more attention for separation purposes. Nanoparticles have large specific surface areas; thus, a large fraction of active sites are available for appropriate chemical interaction.[9–14] In the numerous nanoparticles, magnetic nanoparticles have been widely researched because of their magnetic properties. But the naked magnetic nanoparticles have low adsorption on account of large solute molecules that cannot have specific adsorption. Thus, many organic functional monomers or polymers have been modified on magnetic nanoparticles such as polyacrylic acid,[15] tetrabenzyl,[16] polyacrylamide,[17] diphenyl,[18] phosphatidylcholine,[19] and so on.

Magnetic-assisted sorption separation methods (MSS), a novel form of sorption method, has been developed based on the use of magnetic nanoparticles.[11–20] In MSS methods, functionalized magnetic nanomaterials are dispersed into samples to adsorb target compounds, and then the sorbents are separated rapidly by applying an external magnetic field. Compared with other adsorption methods, the MSS method possess many advantages, including adsorption efficiency and time saving.[11–20] A review of the literature on chiral separation using the method of MSS reveals that few studies have been conducted. Separation of the two enantiomers of racemic *N*-(3,5-dinitrobenzoyl)-α-amino acid *N*-propylamides was studied by Choi and Hyun.[20] Enantioseparation of amino acids enantiomers using β-cyclodextrins functionalized Fe_3O_4 nanospheres was reported by Chen et al. [21]

In this study, *R*(+)α-methylbenzylamine (RMBA)-modified magnetic nanoparticles were synthesized. This was achieved by the interaction of RMBA with 3-glycidoxypropyldimethoxymethylsilane (GLYMO), which was then immobilized on silica-coated magnetic nanoparticles (see Scheme 1). Synthesized magnetic chiral sorbent (RMBAG-SCMPs) was used as a chiral selector for the magnetic separation of mandelic acid enantiomers.

To the best of our knowledge, this is the first report concerning the use of RMBA-modified magnetic nanoparticles as a magnetic chiral material to magnetically separate mandelic acid enantiomers.

EXPERIMENTAL METHODS

Materials

3-Glycidoxypropyldimethoxymethylsilane (GLYMO, 98%), tetraethylorthosilicate (TEOS), *R*(+)α-methylbenzylamine (RMBA, 98%), racemic

*Correspondence to: B. Tural, Department of Chemistry, Faculty of Education, Dicle University, 21280, Diyarbakir, Turkey.
E-mail: bilsentural@gmail.com
Received for publication 1 April 2015; Accepted 6 August 2015
DOI: 10.1002/chir.22524
Published online in Wiley Online Library (wileyonlinelibrary.com).

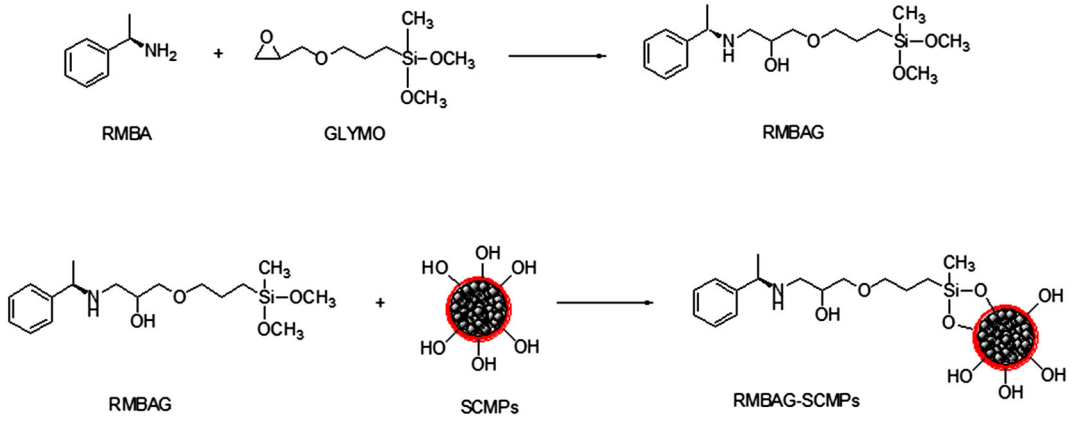

Scheme 1. Schematic illustration for the preparation steps of R(+)α-methylbenzylamine (RMBA) functionalized SCMPs.

mandelic acid (rac.-MA), *(R)-(−)*-mandelic acid (*R*-MA), and *(S)-(+)*-mandelic acid (*S*-MA) were obtained from Sigma Chemical (St. Louis, MO). All aqueous solutions were prepared with deionized water that had been passed through a Millipore (Bedford, MA) milli-Q Plus water purification system.

Characterization Techniques

Magnetization measurements were conducted using a vibrating sample magnetometer (VSM) (Quantum Design PPMS-9T) at room temperature. The size and morphology of the silica-coated magnetite nanoparticles (SCMPs) were investigated using transmission electron microscopy (TEM) (JEOL 2100 F, Japan). For TEM analysis, the SCMPs were redispersed in pure water by sonication for 10 s and a drop of suspension was placed onto SPI Double Copper Grids 100/200. Fourier-transformed infrared (FT-IR) spectra were measured on a Thermo Scientific Nicolet IS10 FT-IR spectrometer (Pittsburgh, PA). Sixteen scans were collected at a resolution of 4 cm^{-1}. The particle sizes and distributions of the SCMPs and RMBAG-SCMPs were determined by using the Dynamic Light Scattering Technique (Zeta Sizer Nano-ZS, Malvern, PA). The measurement temperature was kept at 25°C.

Synthesis of RMBA Functionalized SCMPs

Synthesis of SCMPs was previously reported by our group.[11–13] We utilized a two-step postgraft method in order to synthesize the RMBA functionalized magnetic nanoparticles (Scheme 1). GLYMO and RMBA were reacted to prepare RMBA-bonded GLYMO (denoted RMBAG). After dissolving 46.7 μL of RMBA in 20 mL of deionized water, the pH value of the solution was measured and obtained at 9.5. To minimize the hydrolysis of GLYMO, the solution was transferred into a flask bottle placed in an ice-bath at 0°C, and 40 μL of GLYMO was slowly added into the RMBA solution while continuously stirring the mixture. The temperature of the mixed solution was raised to 40°C and it was stirred for 6 h and subsequently was placed into an ice-bath for 5 min to decrease the temperature to 0°C. After adding another 40μL of GLYMO, the temperature of the mixed solution was raised to 65°C and stirred for 6 h. Finally, the prepared RMBAG solution was adjusted to pH 6 with concentrated HCl. To obtain surface functionalized magnetic particles, 30 mg of the SCMPs were mixed with 10 mL of the prepared RMBAG solution in a flask at 75°C for 2 h with stirring, and then the suspension was separated with the help of a permanent magnet, the supernatant was removed, and RMBA functionalized SCMPs, denoted as RMBAG-SCMPs (Scheme 1).

Sorption Experiments

To verify the enantioseparation capacity of RMBAG-SCMPs for mandelic acid enantiomers, sorption experiments were carried out batchwise to examine the effect of contact time, sorbent dosage, and initial concentration of rac.-MA. The experiments were conducted with 90 mg of RMBAG-SCMPs and 10 mL rac.-MA solutions within the range of 2.5–30 mM at 25°C. The mixtures were shaken on a shaking incubator at a constant agitation speed of 120 rpm for 45 min. After the magnetic separation process, 0.5 mL of sample was taken from the clear part to be extracted with 5 mL of diethyl ether five times (using 1 mL of diethyl ether each time). After mandelic acid had been contained in the ether phase, ether was evaporated. The hexane/isopropanol mixture, which had been prepared previously (at a ratio of 1/1), was added to the rest solid and analyzed by HPLC using a CHIRALPAK AD-H column and n-hexane/isopropanol/trifluoro acetic acid (80/20/0.1) as mobile phase at a 0.8 mL/min flow rate at 25°C. The detection wavelength was 254 nm and each injection volume was 20 μL.

The selectivity for enantioseparation was calculated in terms of the percentage enantiomeric excess (%*ee*) of the samples:

$$e.e.(\%) = \frac{S_R - S_S}{S_R + S_S} \times 100 \quad (1)$$

Where S is the S-enantiomer peak area and R is the R-enantiomer peak area obtained from HPLC.

RESULTS AND DISCUSSION

Characterization

The FT-IR spectra of the SCMPs and the RMBAG-SCMPs are shown in Figure 1 together with the spectrum for pure RMBA molecules. Abroad absorption bands in the range of 900–1200 cm^{-1} observed in the FT-IR spectrum (Fig. 1A,B) is assignable to the Si-O, Si-O-C, Si-O-Fe, and Si-O-Si bonds.[22] After the SCMPs surface modification with RMBA, a characteristic peak appears at 3365 cm^{-1}. It is ascribed to N-H stretching band from RMBA (see spectra RMBA (Fig. 1C) and RMBAG-SCMPs (Fig. 1A)).[23] Some alkyl C–H and aryl C–H absorption bands at about 2800–3000 cm^{-1} were detected for the RMBAG-SCMPs and pure RMBA. A peak at around ~1450 cm^{-1} assigned to C-N deformation were clearly visible in the spectra of the modified nanoparticle (Fig. 1A) and pure RMBA (Fig. 1C). The results indicate that RMBA was attached successfully to the surface of the SCMPs (Fig. 1).[23]

The magnetic properties of the Fe_3O_4 (MNPs) and the RMBAG-SCMPs were investigated by VSM analysis at room temperature. The saturation magnetization of pure magnetite nanoparticles (Fig. 2A) and the chitosan-magnetite

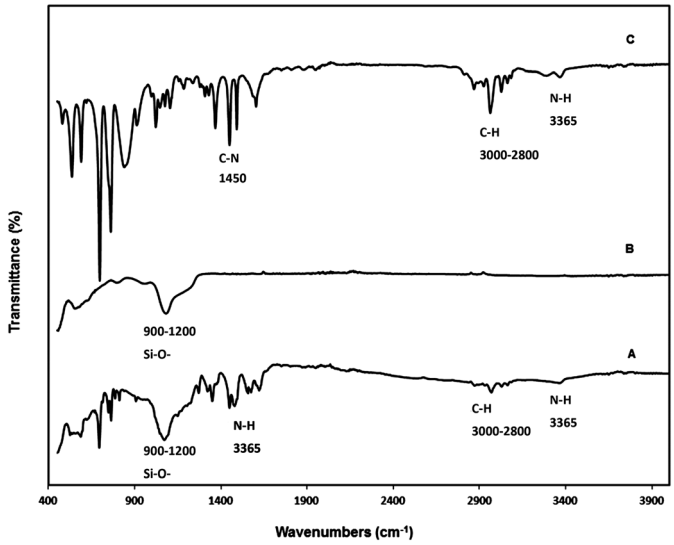

Fig. 1. FT-IR spectra of silica coated magnetite particles (SCMPs) **(B),** the nanoparticles reacted with RMBA (RMBAG-SCMPs) **(A),** and with the spectrum of pure RMBA molecules **(C).**

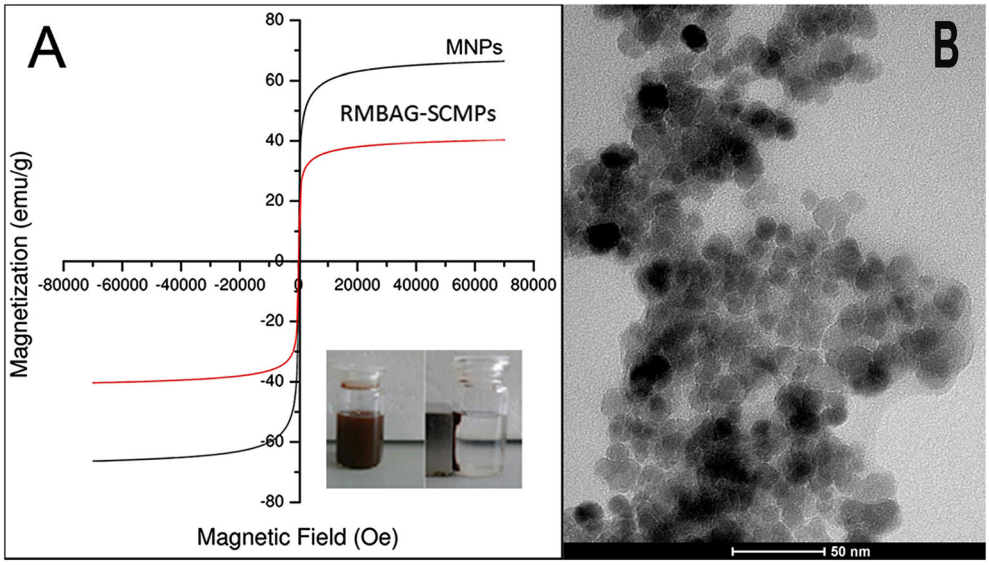

Fig. 2. (**A)** Magnetization versus magnetic field for the RMBAG-SCMPs, (**B)** TEM graphs of the RMBAG-SCMPs

nanocomposites (Fig. 2A) were about 68.0 emu g^{-1} and to be 37.0 emu $g^{-}1$, respectively. The decrease in the saturation magnetization of nanoparticles after surface modification can be explained by the decrease in the amount of the magnetic moments per unit weight due to the diamagnetic contribution of silica shell and RMBA. As can be seen from the insert in Figure 2A, this saturation magnetization of RMBAG-SCMPs makes them very susceptible to magnetic fields, and therefore makes the solid and liquid phases easily separated.[14]

The TEM brightfield micrograph for the RMBAG-SCMPs is shown in Figure 2B. As can be seen from the TEM image, the average size of the particles is ~10 nm.

The particle agglomeration size distributions of the SCMPs and RMBAG-SCMPs are shown in Figure 3. Z-average particle size and poly-dispersitivity index (PDI) of the SCMPs were determined as 595 nm and 0.378, respectively, and Z-average particle size and PDI of the RMBAG-SCMPs were determined as 1060 nm and 0.397, respectively. These results suggest that the particle size of the SCMPs was increased significantly (from 595 nm to 1060 nm) when they were functionalized with RMBA.

Sorption Studies

The separation of the enantiomers of rac.-MA onto RMBAG-SCMPs as a function of contact time is shown in Figure 4A,B. It can be seen that the amount of *R*-MA and *S*-MA sorbed per unit mass of RMBAG-SCMPs increased with the increase of initial concentration. The sorption equilibrium was achieved at 45 min for each of the enantiomers of rac.-mandelic acid. It can be seen that each of the enantiomers of chiral mandelic acid sorption onto RMBAG-SCMPs is fast in the first 20 min and then it becomes slower near equilibrium. Equilibrium was reached after 45 min. This

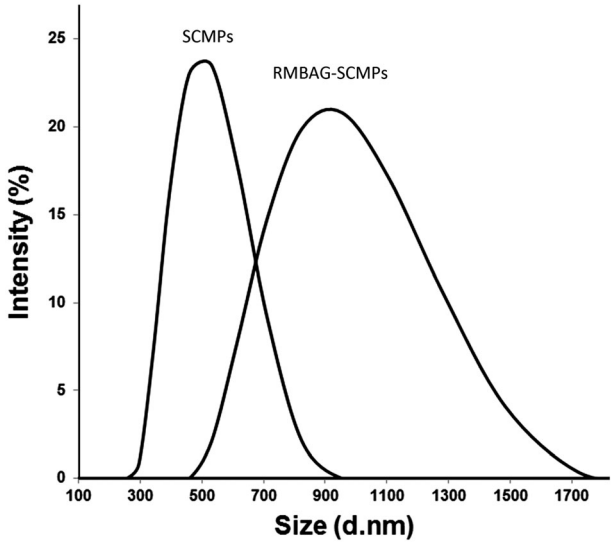

Fig. 3. Z-average particle size distribution for the SCMPs and RMBAG-SCMPs.

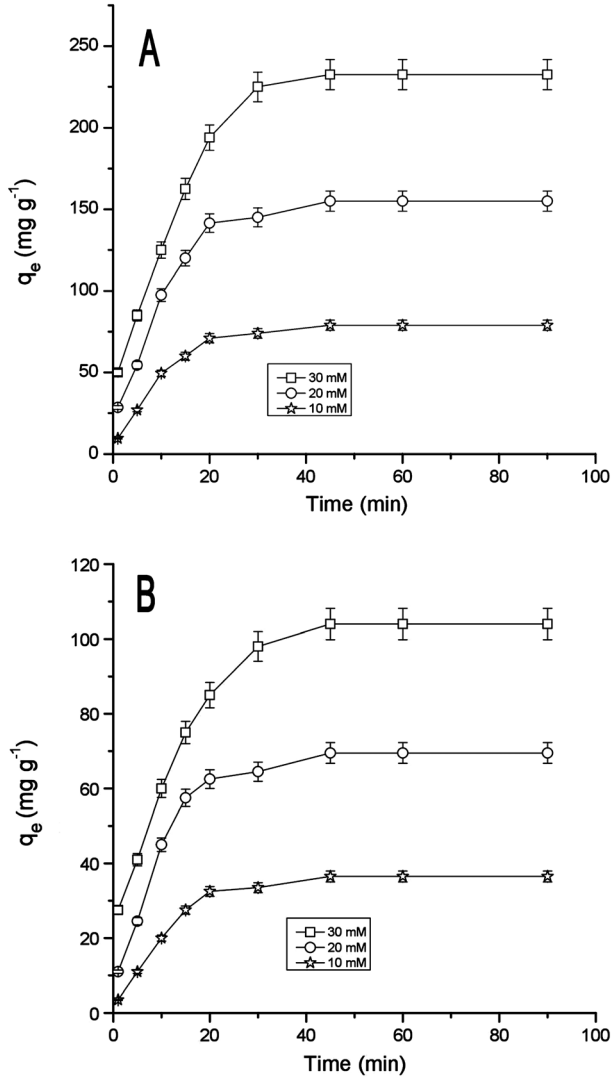

Fig. 4. Effect of agitation time on sorption capacity (q_e, mg g^{-1}) of racemic mandelic acid **(A)** *S*-MA **(B)** *R*-MA on RMBAG-SCMPs at 10, 20, and 30 mM initial concentrations of racemic mandelic acid.

can be explained by the large number of available vacant sites on the RMBAG-SCMPs surfaces, which are gradually occupied in time as a result of the sorption process.[10] The sorption order is *S*-MA > *R*-MA.

The effect of RMBAG-SCMPs dose on the separation of the *R*-MA and *S*-MA is demonstrated in Figure 5A,B. From this figure it is evident that the percentage sorption of *R*-MA and *S*-MA onto RMBAG-SCMPs increases with the increase in RMBAG-SCMPs dose, while the sorption capacity, *qe* (mg/g), at equilibrium decreases. This can be attributed to the increased sorbent surface area and availability of more sorption sites of sorbent. It is apparent that the uptake of solute markedly increased up to a chiral sorbent dose of 90 mg and thereafter no significant increase was observed. Hence, the excellent sorption of *R*-MA and *S*-MA can be obtained by using 110 mg of RMBAG-SCMPs. It was observed that RMBAG-SCMPs had an affinity towards the *R*-MA and *S*-MA with different percentages. Hence, RMBAG-SCMPs stood out with a remarkable selective sorption. As can be seen in Figures 5, the (*R)*-MA was sorbed with 41%, whereas the (S)-MA was sorbed with 74% by 90 mg RMBAG-SCMPs. These findings clarify that RMBAG-SCMPs has sorption affinity towards enantiomers of rac.-MA. The sorption mechanism

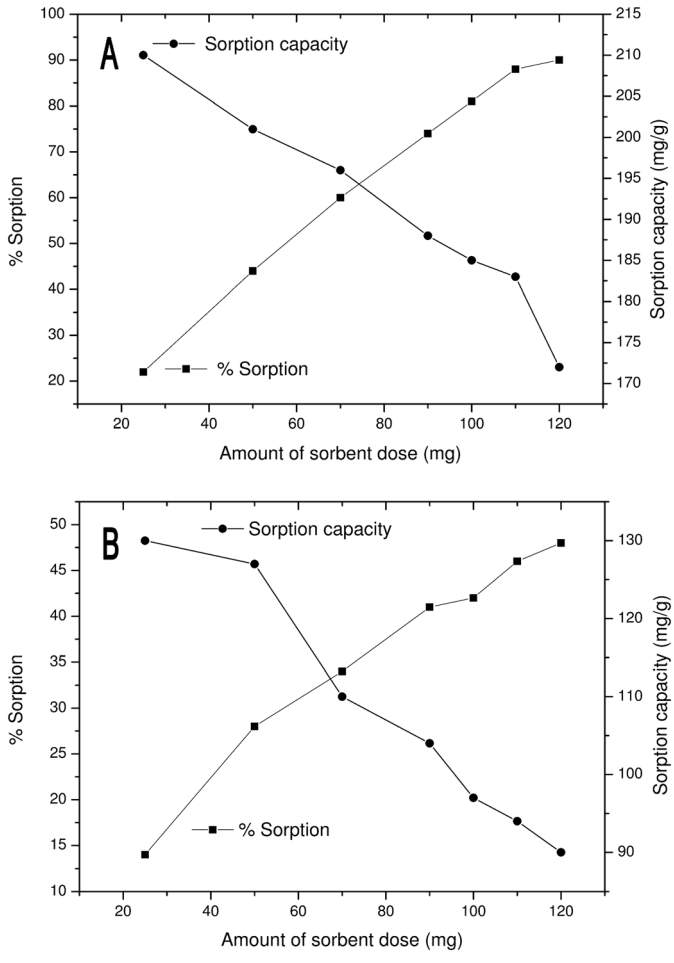

Fig. 5. Effect of sorbent dose for sorption of racemic mandelic acid enantiomers on RMBAG-SCMPs using 30 mM rac.-MA at 45 min agitation time **(A)** percent removal and sorption capacity (mg g^{-1}) of S-MA. **(B)** Percent removal and sorption capacity (mg g^{-1}) of R-MA.

might proceed by forming significant hydrogen bonding and host–guest interaction between the mandelic acid and RMBAG-SCMPs.

Table 1 shows the influence of the initial concentration of rac.-MA and RMBAG-SCMPs dose on the optical resolution. When the initial concentration of rac.-MA increased from 5 to 30 mM, the percent of *ee* decreased from 43% to 39%. This was probably because more and more active sites became covered by the isomer, thus leading to permeation of the other isomer.[1,5,24] Therefore, the amount of sorbent dose was increased from 90 mg to 120 mg (Table 1). The %*ee* increases with the increase in chiral sorbent dose from 90 mg to 110 mg. A subsequent increment of dose formed a small increase in *ee*. Therefore, the best enantioselectivity of RMBAG-SCMPs was obtained by using 30 mM rac.-MA and 110 mg RMBAG-SCMPs at 45 min and 25°C. HPLC chromatograms showing the best *ee* value are shown in Figure 6, including that of before and after separation by magnetic assisted sorption. As can be seen from Figure 6, the best *ee* value was obtained as 64%.

Sorption Isotherms

The equilibrium isotherms are used to describe the sorbate–sorbent interactions, and their knowledge is important from both a theoretical and a practical point of view. Various isotherm models have been published in the literature to express experimental data sorption isotherms. In the present study, Langmuir, Freundlich, and Dubinin-Radushkevich isotherms were employed.

The basic assumption of Langmuir isotherm is based on monolayer coverage of the sorbate on the homogeneous surface of the sorbent.[25] The linear form of the Langmuir isotherm equation is expressed as:[26]

$$\frac{1}{q_e} = \frac{1}{Q_m} + \frac{1}{Q_m K_L} \cdot \frac{1}{C_e} \tag{2}$$

where C_e is the equilibrium concentration of sorbate (mg L^{-1}), q_e (mg/g) is the amount of enantiomers of rac.-MA sorbed per unit mass of sorbent, Q_m the maximum sorption capacity (mg g^{-1}), and K_L is the constant associated with the free energy of sorption (L mg^{-1}). Where Q_m and K_L can be determined from the linear plot of $1/q_e$ versus $1/C_e$ (Table 2).

The Freundlich isotherm model is used to describe the sorption characteristics for the heterogeneous sorbent surface with sites that have diverse energies of sorption. Hence, the Freundlich equation can be written as the logarithmic form[27]

$$Log q_e = Log K_F + \frac{1}{n} Log C_e \tag{3}$$

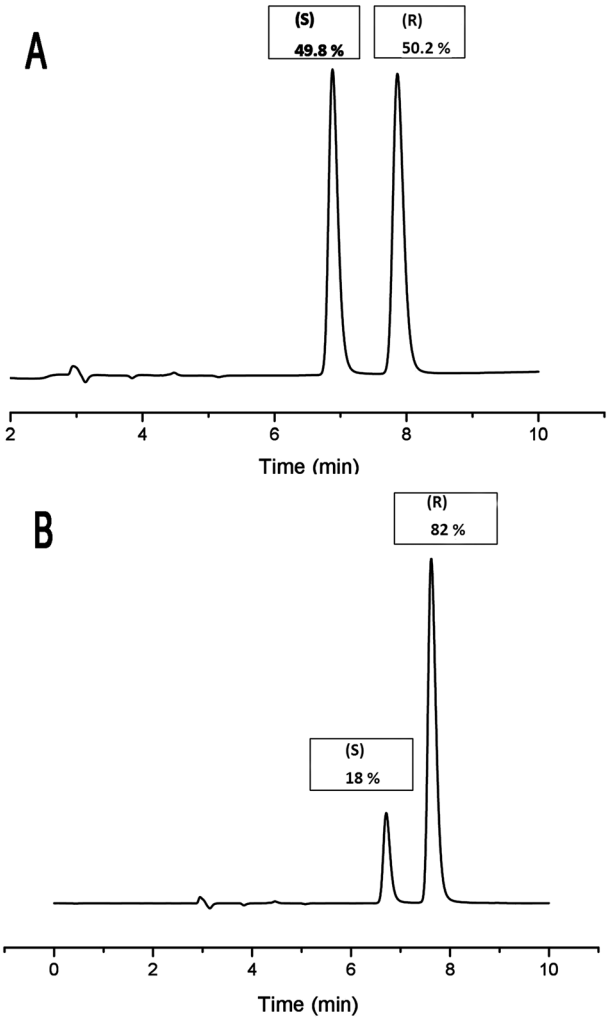

Fig. 6. HPLC chromatogram (% area) of racemic mandelic acid before (**A**) and after (**B**) separation by magnetic assisted sorption carried out on Chiralpak AD-H column and n-hexane/isopropanol/trifluoro acetic acid (80/20/0.1) as mobile phase at 0.8 mL/min flow rate at 25°C. The detection wavelength was 254 nm and each injection volume was 20 μL.

TABLE 1. Enantiomeric excess values of racemic mandelic acid[a]

	rac-MA		Adsorbed Amount		Residual Amount		
Dose (mg)	C_o (mM)	C_o (mg/10mL)	S-MA(mg)	R-MA (mg)	S-MA (mg)	R-MA (mg)	[a]*ee* %
90	5	7.6	3.0	1.7	0.8	2.1	43
90	10	15.2	5.8	3.3	1.8	4.3	41
90	15	22.8	8.6	4.8	2.9	6.6	40
90	20	30.4	11.3	6.3	4.0	9.0	39
90	25	38.0	14.1	7.8	5.0	11.2	39
90	30	45.6	16.9	9.4	5.9	13.5	39
100	30	45.6	18.5	9.6	4.3	13.2	51
110	30	45.6	20.1	10.5	2.7	12.3	64
120	30	45.6	20.5	10.5	2.3	12.3	67

[a]Enantiomeric excess was checked with HPLC chiral column (CHIRALPAK AD-H).
Mobile phase: n-hexane/isopropanol/trifluoro acetic acid (80/20/0.1).
Flow rate: 0.8 ml/min. Temperature: 25°C. Detector: 254 nm DAD. C_o: initial concentration of rac-MA; volume is 10mL for each experiment.

TABLE 2. Isotherms parameters for the sorption of racemic mandelic acid enantiomers on RMBAG-SCMPs

Adsorbates	Langmuir constants			Freundlich constants				Dubinin–Raduskvich Isotherm			
	qm (mg g^{-1})	KL (L/mg)	qm, exp. (mg g^{-1})	R^2	KF (L/g)	n	R^2	K (mol^2/kJ)	qm (mol/g)	E ($kJmol^{-1}$)	R^2
(*R*)-(–) MA	167	6.9E-03	114	0.94	3.08	1.54	0.91	2E-04	90.6	0.89	0.80
(*S*)- (+) MA	238	0.268	188	0.98	52	1.98	0.83	2.93	169	0.29	0.86

where q_e is the amount of enantiomers of rac.-MA sorbed per unit mass of sorbent in equilibrium (mg/g) and C_e is 1liquid phase concentration of rac.-MA enantiomers in equilibrium (mg L^{-1}). The constant K_F ($mg^{1-(1/n)}$ $L^{1/n}$ g^{-1}) is an approximate indicator of sorption capacity, while $1/n$ is a function of the strength of sorption in the sorption process. The values of K_F and n were obtained by plotting Log(q_e) vs. Log(C_e) and given in Table 2. The n value shows the degree of nonlinearity between solution concentration and sorption as follows: if $n = 1$, then sorption becomes linear; if $n < 1$, then sorption becomes a chemical process; if $n > 1$, then sorption becomes a physical process.[28] As can be seen in Table 2, since n values of *R*-MA and *S*-MA were calculated as 1.54 and 1.98, respectively, the sorption of *R*-MA and *S*-MA on RMBAG-SCMPs is a physical process.[29]

Langmuir and Freundlich sorption constants and correlation coefficients (R^2) are presented in Table 2. In both cases, linear plots were gained, which reveal the applicability of these isotherms on the ongoing sorption process. The results revealed that Langmuir sorption isotherm was a more linear model than Freundlich for the sorption of mandelic acid enantiomers on RMBAG-SCMPs because correlation Langmuir coefficients (R^2) are greater than Freundlich. The important features of the Langmuir sorption isotherm parameter can be used to foresee the affinity between the sorbates and sorbent using a dimensionless constant called a separation factor or equilibrium parameter (R_L), which is expressed by the following relationship[26,30]

$$R_L = \frac{1}{1 + bC_0} \tag{4}$$

where b (L/mg) is the Langmuir constant and C_0 (mg/L) is the initial concentration of mandelic acid enantiomers. The value of R_L indicated the type of Langmuir isotherm to be irreversible ($R_L = 0$), linear ($R_L = 1$), unfavorable ($R_L > 1$), or favorable ($0 < R_L < 1$).[26,30] The R_L values between 0 and 1 indicate favorable sorption. The R_L value in the present investigation was found to be between 0.80 and 0.95 for *R*-MA and *S*-MA, indicating that the sorption of the *R*-MA and *S*-MA on RMBAG-SCMPs is favorable.

A Dubinin–Radushkevich (D-R) isotherm was also applied to estimate the porosity apparent free energy and the characteristics of sorption.[31–33] It can be used to describe sorption on both homogenous and heterogeneous surfaces. The D–R equation can be defined by the following equation[33,34]

$$\ln q_e = \ln q_{\max} - \beta\varepsilon^2 \tag{5}$$

where $q_{\max}$ the theoretical saturation capacity, β is a constant related to the sorption energy, ε the Polanyi potential (mol^2/J^2), calculated from Eq.:[6]

$$\varepsilon = RT\ln\left[1 + \frac{1}{C_e}\right] \tag{6}$$

where T is the solution temperature (K), R is the gas constant (8.314 J mol^{-1} K^{-1}), and C_e is the equilibrium concentration of sorbate (mg L^{-1}). By plotting ln q_e versus ε^2, it is possible to determine the value of β from the slope and the value of q_{max} (mg g^{-1}) from the intercept, which is ln q_{max}. The value of mean free sorption energy, E (kJ/mol), can be estimated by using B values as expressed in the following equation from D–R parameter B as follows[35]

$$E = \frac{1}{\sqrt{2B}} \tag{7}$$

The extent of E is useful for guessing the type of sorption reaction. If E is in the range of 8–16 kJ/mol, sorption is ruled by chemical ion-exchange. In the case of E < 8 kJ/mol, physical forces may affect the sorption.[36] The parameters obtained using Eqs. (6, 7) are evaluated in Table 2. The E values calculated using Eq. [7] is 0.89 and 0.29 kJ mol^{-1} for the *R*-MA and *S*-MA, respectively. This indicates that physico-sorption played a significant role in the sorption of the *R*-MA and *S*-MA onto RMBAG-SCMPs.

Sorption Kinetics

The sorption kinetics of *R*-MA and *S*-MA onto RMBAG-SCMPs were investigated by fitting the experimental data with two kinetic models, namely, pseudo-first-order and pseudo-second-order. The pseudo-first-order equation and pseudo-second-order equation as expressed as[37,38]

$$\ln(q_e - q_t) = \ln q_e - k_1 t \tag{8}$$

$$\frac{t}{q_t} = \frac{1}{k_2 q_e^2} + \left(\frac{1}{q_e}\right)t \tag{9}$$

Here, q_t is the amount of mandelic acid enantiomers sorbed at time t (mg/g), q_e is the amount of mandelic acid enantiomers sorbed at equilibrium, k_1 is the sorption rate constant (min^{-1}) for the first order sorption, and k_2 the pseudo-second-order rate constant. The rate constants k_1, k_2 and q_e were calculated from the slopes and intercepts of the linear plot of ln($q_e - q_t$) or t/q_t against t, respectively. Comparative linear first-order and second-order sorption rate constants, calculated q_e, experimental q_e and R^2 values are given for *R*-MA and *S*-MA at 30°C in Table 3.

It can be seen that the linear correlation coefficients for the first-order and second-order model are good and based on the

TABLE 3. Kinetic parameters of rac.-mandelic acid enantiomers on RMBAG-SCMPs

	Pseudo-first-order				Pseudo-second-order		
	q(e, exp) (mg g^{-1})	K_1 (min^{-1})	q(e, cal) (mg g^{-1})	R^2	K_2 (g mg^{-1} min^{-1})	q(e, cal) (mg g^{-1})	R^2
(*R*)-(-) MA (mM)							
30	104	0.087	97.3	0.98	1.14E-03	125	0.99
20	69.5	0.092	60.3	0.95	2.09E-03	76.9	0.99
10	36.5	0.089	36.4	0.95	2.58E-03	41.6	0.99
(*S*)-(+) MA(mM)							
30	188	0.086	154	0.98	1.01E-03	200	0.99
20	95	0.085	70.3	0.95	2.18E-03	101	0.99
10	64	0.096	59.4	0.95	2.32E-03	69.9	0.99

comparison between experimental and theoretically calculated q_e values, it was found that the pseudo-second-order model fitted better than the pseudo-first-order model for sorption process.

CONCLUSION

We have presented a simple and convenient chemical method for the preparation of RMBAG-SCMPs using RMBA as a chiral selector to conduct the enantiomeric separation of rac.-MA enantiomers. The method using RMBA-modified magnetic nano-sorbent effectively separates mandelic acid enantiomers. The sorption capacity of mandelic acid enantiomers onto the RMBAG-SCMPs depended on contact time, the initial concentration of mandelic acid enantiomers, and sorbent dose. The sorption capacity increased with an increase in the initial concentration of mandelic acid enantiomers. Kinetic studies have shown that the reaction of sorption is pseudo-second-order. The values of thermodynamic parameters obtained for the sorption process indicated that the Langmuir isotherm model fitted quite well with the experimental data (correlation coefficient $R^2 \geq 0.94$), compared with the other two isotherm models. The maximum adsorption capacity of rac.-MA on the RMBAG-SCMPs was found to be 405 mg g^{-1}. The enantioseparation of (*R*)-(−)-mandelic acid (*ee*, 64%) was achieved by using 110 mg magnetic chiral sorbent and 10 mL 30 mM rac.MA at 45 min and at 25°C.

Even though the complete separation of the two enantiomers was not achieved in this study, the method of magnetic field induced separation of enantiomers with the use of SCMPs tagged to an appropriate chiral selector is expected to be developed further and utilized as a successful enantiomer separation technique in the future.

ACKNOWLEDGMENTS

This project is funded by the financial support from Dicle University Research Fund (DUBAP, Project No. 13-ZEF-28, Project No. 13-ZEF-85 and Project No. 10-ZEF-28).

LITERATURE CITED

1. Mayani VJ, Abdi SHR, Kureshy RI, Khan NH, Agrawal S, Jasra RV. Synthesis and characterization of mesoporous silica modified with chiral auxiliaries for their potential application as chiral stationary phase. J Chromatogr A 2008;1191:223–230.
2. Wang P, Zhang E, Niu J-F, Ren Q-H, Zhao P, Liu H-M. An excellent new resolving agent for the diastereomeric resolution of rac-mandelic acid. Tetrahedron: Asymmetry 2012;23:1046–1051.
3. West C, Bouet A, Gillaizeau I, Coudert G, Lafosse M, Lesellier E. Chiral separation of phospine-containing α-amino acid derivatives using two complementary cellulosic stationary phases in supercritical fluid chromatography. Chirality 2010;22:242–251.
4. Yokota M, Doki N, Shimizu K. Chiral separation of a racemic compound induced by transformation of racemic crystal structures: dl-glutamic acid. Cryst Growth Des 2006;6:1588–1590.
5. Mayani VJ, Abdi SHR, Kureshy RI, Khan NH, Agrawal S, Jasra RV. Synthesis and characterization of (S)-amino alcohol modified M41S as effective material for the enantioseparation of racemic compounds. J Chromatogr A 2006;1135:186–193.
6. Kacprzak K, Maier N, Lindner W. Unexpected enantioseparation of mandelic acids and their derivatives on 1,2,3-triazolo-linked quinine tert-butyl carbamate anion exchange-type chiral stationary phase. J Sep Sci 2010;33:2590–2598.
7. Maier NM, Lindner W. Chirality in drug research. Wiley VCH: Weinheim, Germany; 2006. p 189.
8. Lämmerhofer M. Chiral recognition by enantioselective liquid chromatography: mechanisms and modern chiral stationary phases. J Chromatogr A 2010;1217:814–856.
9. Wu W, He Q, Jiang C. Magnetic iron oxide nanoparticles: synthesis and surface functionalization strategies. Nanoscale Res Lett 2008;3:397–415.
10. Tural S, Tural B, Ece MŞ, Yetkin E, Özkan N. Kinetic approach for the purification of nucleotides with magnetic separation. J Sep Sci 2014;37:3370–3376.
11. Tural B, Şimşek İ, Tural S, Çelebi B, Demir AS. Carboligation reactivity of benzaldehyde lyase (BAL, EC 4.1.2.38) covalently attached to magnetic nanoparticles. Tetrahedron: Asymmetry 2013;24:260–268.
12. Tural B, Tural S, Demir AS. Carboligation reactions mediated by benzoylformate decarboxylase immobilized on a magnetic solid support. Chirality 2013;25:415–421.
13. Tural B, Tural S, Ertaş E, Yalınkılıç İ, Demir AS. Purification and covalent immobilization of benzaldehyde lyase with heterofunctional chelate-epoxy modified magnetic nanoparticles and its carboligation reactivity. J Mol Catal B: Enzym 2013;95:41–47.
14. Ma Z, Guan Y, Liu H. Superparamagnetic silica nanoparticles with immobilized metal affinity ligands for protein adsorption. J Magn Mater 2006;301:469–477.
15. Liao MH, Chen DH. Fast and efficient adsorption/desorption of protein by a novel magnetic nano-adsorbent. Biotechnol Lett 2002;24:1913–1917.
16. Zou Y, Chen YZ, Yan ZH, Chen CY, Wang JP, Yao SZ. Magnetic solid-phase extraction based on tetrabenzyl modified Fe_3O_4 nanoparticles for the analysis of trace polycyclic aromatic hydrocarbons in environmental water samples. Analyst 2013;138:5904–5912.
17. Xiong L, Jiang HW, Wang DZ. Preparation and characterization of polyacrylamide-modified Fe_3O_4 magnetic nanoparticles. Acta Polymer Sin 2008;3:259–265.
18. Bianchi F, Chiesi V, Casoli F, Luches P, Nasi L, Careri M, Mangia A. Magnetic solid-phase extraction based on diphenyl functionalization of Fe_3O_4 magnetic nanoparticles for the determination of polycyclic aromatic hydrocarbons in urine samples. J Chromatogr B 2012;1231:8–15.
19. Zhang SX, Niu HY, Zhang YY, Liu JS, Shi YL, Zhang XL, Cai YQ. Biocompatible phosphatidylcholine bilayer coated on magnetic nanoparticles and their application in the extraction of several polycyclic aromatic hydrocarbons from environmental water and milk samples. J Chromatogr A 2012;1238:38–45.

20. Choi HJ. Hyun MH. Separation of enantiomers with magnetic silica nanoparticles modified by a chiral selector: enantioselective fishing. Chem Commun 2009; 6454–6456.
21. Chen X, Rao J, Wang J, Gooding JJ, Zou G, Zhang Q. A facile enantioseparation for amino acids enantiomers using β-cyclodextrins functionalized Fe_3O_4 nanospheres. Chem Commun 2011;47:10317–10319.
22. Liu G, Wu H, Zheng H, Tang L, Hu H, Yang H, Yang S. Synthesis and applications of fluorescent-magnetic-bifunctional dansylated Fe_3O_4@SiO_2 nanoparticles. J Mater Sci 2011;46:5959–5968.
23. Palaprat G, Marty J-D, Routaboul C, Lattes A, Mingotaud A-F, Mauzac M. Study of hydrogen bonding in liquid crystalline solvent by Fourier transform infrared spectroscopy. J Phys Chem A 2006;110:12887–12890.
24. Tian F-Y, Zhang J-H, Duan A-H, Wang B-J, Yuan L-M. Chiral separation of D,L-mandelic acid using an enantioselective membrane formed by polycondensation of β-cyclodextrin with 1,6-diisocyanatohexane on a polysulfone membrane. J Membr Sep Tech 2012;1:72–78.
25. Langmuir I. The adsorption of gases on plane surfaces of glass, mica and platinum. J Am Chem Soc 1918;40:1361–1403.
26. Hameed BH, Rahman AA. Removal of phenol from aqueous solutions by adsorption onto activated carbon prepared from biomass material. J Hazard Mater 2008;160:576–581.
27. Freundlich H. Über die Adsorption in Lösungen. Wilhelm Engelmann: Germany; 1906.
28. SenthilKumar P, Ramalingam S, Abhinaya RV, Kirupha SD, Vidhyadevi T, Sivanesan S. Adsorption equilibrium, thermodynamics, kinetics, mechanism and process design of zinc(II) ions onto cashew nut shell. Can J Chem Eng 2012;90:973–982.
29. Kinniburgh DG. General purpose adsorption isotherms. Environ Sci Technol 1986;20:895–904.
30. Kumar NS, Suguna M, Subbaiah MV, Reddy AS, Kumar NP, Krishnaiah A. Adsorption of phenolic compounds from aqueous solutions onto chitosan-coated perlite beads as biosorbent. Ind Eng Chem Res 2010;49:9238–9247.
31. Dubinin MM. The potential theory of adsorption of gases and vapors for adsorbents with energetically nonuniform surfaces. Chem Rev 1960;60:235–241.
32. Dubinin MM. Modern state of the theory of gas and vapour adsorption by microporous adsorbents. Institute of Physical Chemistry: U.S.S.R. Academy of Sciences, Moscow; 1965. p 309–322.
33. Dubinin MM, Radushkevich LV. Equation of the characteristic curve of activated charcoal. Proc Acad Sci USSR Phys Chem Sect 1947; 331–333.
34. Gregg SJ, Sing KSW. Adsorption, surface area, and porosity. Academic Press: London, New York; 1982.
35. Benhammou A, Yaacoubi A, Nibou L, Tanouti B. Adsorption of metal ions onto Moroccan stevensite: kinetic and isotherm studies. J Colloid Interface Sci 2005;282:320–326.
36. Hongxia Z, Chuanxi W, Zuyi T, Wangsuo WJ. Effects of nitrate, fulvate, phosphate, phthalate, salicylate and catechol on the sorption of uranyl onto SiO2: a comparative study. Radioanal Nucl Chem 2011;287:13–20.
37. Ahmed MJ, Dhedan SK. Equilibrium isotherms and kinetics modeling of methylene blue adsorption on agricultural wastes-based activated carbons. Fluid Phase Equilib 2012;317:9–14.
38. Elwakeel KZ. Removal of reactive black 5 from aqueous solutions using magnetic chitosan resins. J Hazard Mater 2009;167:383–392.